IEEE Access
Multidisciplinary | Rapid Review | Open Access Journal

Received March 9, 2020, accepted April 2, 2020, date of publication April 14, 2020, date of current version May 6, 2020.

Digital Object Identifier 10.1109/ACCESS.2020.2987970

Decentralized Greedy-Based Algorithm for Smart Energy Management in Plug-in Electric Vehicle Energy Distribution Systems

ABBAS MEHRABI[1], (Member, IEEE), H. S. V. S. KUMAR NUNNA[2], (Member, IEEE), ARESH DADLANI[2], (Member, IEEE), SEUNGPIL MOON[3], AND KISEON KIM[4], (Senior Member, IEEE)

[1]Department of Computing and Technology, Nottingham Trent University, Nottingham NG11 8NS, U.K.
[2]Department of Electrical and Computer Engineering, Nazarbayev University, Astana 010000, Kazakhstan
[3]Korea Electric Power Research Institute (KEPRI), Deajeon 34056, South Korea
[4]School of Electrical Engineering and Computer Science, Gwangju Institute of Science and Technology, Gwangju 61005, South Korea

Corresponding author: Abbas Mehrabi (abbas.mehrabidavoodabadi@ntu.ac.uk)

This work was supported by the Ministry of Oceans and Fisheries, South Korea, under the part of the project titled "Development of Automatic Identification Monitoring System for Fishing Gears."

ABSTRACT Variations in electricity tariffs arising due to stochastic demand loads on the power grids have stimulated research in finding optimal charging/discharging scheduling solutions for electric vehicles (EVs). Most of the current EV scheduling solutions are either centralized, which suffer from low reliability and high complexity, while existing decentralized solutions do not facilitate the efficient scheduling of on-move EVs in large-scale networks considering a smart energy distribution system. Motivated by smart cities applications, we consider in this paper the optimal scheduling of EVs in a geographically large-scale smart energy distribution system where EVs have the flexibility of charging/discharging at spatially-deployed smart charging stations (CSs) operated by individual aggregators. In such a scenario, we define the social welfare maximization problem as the total profit of both supply and demand sides in the form of a mixed integer non-linear programming (MINLP) model. Due to the intractability, we then propose an online decentralized algorithm with low complexity which utilizes effective heuristics to forward each EV to the most profitable CS in a smart manner. Results of simulations on the IEEE 37 bus distribution network verify that the proposed algorithm improves the social welfare by about 30% on average with respect to an alternative scheduling strategy under the equal participation of EVs in charging and discharging operations. Considering the best-case performance where only EV profit maximization is concerned, our solution also achieves upto 20% improvement in flatting the final electricity load. Furthermore, the results reveal the existence of an optimal number of CSs and an optimal vehicle-to-grid penetration threshold for which the overall profit can be maximized. Our findings serve as guidelines for V2G system designers in smart city scenarios to plan a cost-effective strategy for large-scale EVs distributed energy management.

INDEX TERMS Electric vehicle-to-grid (V2G), distributed energy management, mixed integer non-linear programming, greedy-based algorithm, smart cities.

I. INTRODUCTION

Overwhelming environmental concerns have triggered the dramatic shift towards the electrification of public transportation in smart cities [1]. Electric vehicles (EVs), as cost-efficient and eco-friendly substitutes for fossil fuel-operated vehicles, have received significant attention in recent years from both, academia and industry [2]. Currently, there are over 40 different EVs models in the UK with more expected to join the public transportation fleet in near future [3], [4]. Depending on the operation mode, plug-in EVs that operate solely on battery power have advantages over conventional vehicles. Along with the benefits, however, arise new challenges associated with the unprecedented number of EVs being injected into the electricity grid. One primary issue relates to the power grid unreliability and transmission

The associate editor coordinating the review of this manuscript and approving it for publication was Pierluigi Siano.

overhead from uncontrolled energy trading between EVs and the grid at charging stations (CSs) [2], [5]–[10].

Several existing research efforts address issues associated with the charging/discharging of EVs given their profound impact on the load regulation of vehicle-to-grid (V2G) systems [6], [8], [11]–[14]. The bidirectional energy flow between EVs and the grid enables load flattening by shifting the EV charging demands from peak-load periods to the valley intervals [7], [9], [15]. In light of the energy costs at different time intervals and the uncertainty in EV arrivals, smart scheduling solutions are required to not only boost the obtainable profit for EVs, but also ensure the reliability of the power grid infrastructure through ancillary services [8], [10]. Likewise, there are classes of works dedicated to spatial scalability in EV scheduling and are mainly assorted based on the configuration of the aggregators in the system. Non-preemptive charging/discharging of EVs occur either at one CS operated by a single aggregator with complete prior knowledge of the EV energy needs and departure times [8], [10], or at multiple CSs managed by a single aggregator where the scheduling problem is tackled locally [9].

As the main limitation of major studies on EV scheduling, the effective infrastructure and approaches for smart scheduling of a large-scale network of on-move EVs in an energy distribution system are not considered. In this line, Internet of Vehicles (IoVs) along with recent advances in cloud computing and software-defined networking technologies aim to facilitate the decentralization of EV scheduling and the underlying communication infrastructure [16]–[19]. In spite of such advancements, the objective functions investigated mainly target the satisfaction criteria of EV drivers such as waiting time at CSs or merely maximize the profits of EVs. More specifically, the maximization of social welfare of the entire distribution system including multiple spatially-located CSs, each operated by individual aggregators, has been overlooked in the aforementioned works. Under such a setting, the EV owners enjoy the flexibility of selecting stations that yield the most achievable profit.

Aware of the influential energy distribution system variables (such as the number of CSs and the percentage of V2G penetration), it is thus, crucial to select optimal variables that basically improve the operational costs of CSs. Moreover, from the viewpoint of V2G management, it is necessary to jointly optimize the achievable profit for both, EVs and CSs in a controlled manner which, in turn, motivates energy suppliers to invest on the deployment of CSs for energy transmission to EVs. Given the limitations and motivations stated above, the key contributions of this paper are summarized as follows:

- The joint profit maximization of EVs and CSs, i.e., the social welfare, in scheduling the charging/discharging of EVs for a large-scale energy distribution system is formulated as an MINLP optimization problem.
- A novel online and decentralized algorithm is designed that initially solves the CS selection problem using a greedy-based heuristic, therefore, reducing the original intractable MINLP problem to a tractable form.
- Furthermore, the algorithm then determines the energy trading between the EV and power grid at the selected CS by solving the tractable problem using standard optimization solver with the objective of providing desired ancillary services to the power grid.
- As confirmed by our analytical investigations, the proposed algorithm which is based on greedy approach achieves the efficient solutions within a shorter running time compared to sophisticated solutions which rely on branch and bound (BB) or iterative mechanisms.

Results from simulations conducted on the IEEE 37 bus distribution network reveal that under the best-case performance, the proposed algorithm outperforms a baseline solution in terms of social welfare by about 30% on average and the flatness of final grid electricity load by about 20%. The results also exhibit the optimal number of deployed stations and V2G penetration in the system for which EV owners obtain maximum profit. Our findings can serve as guidelines for V2G designers in smart cities to optimize the operational costs incurred in large-scale distributed CS planning.

The rest of this paper is organized as follows. In Section II, the related works are discussed. The system overview and notations used in system modeling are given in Section III, followed by the optimization problem in Section IV. In Section V, the design and computational complexity of the proposed algorithm is presented. Simulation results are given in Section VI. Finally, the main discussions and conclusion are drawn in Section VII and Section VIII, respectively.

II. RELATED WORK

A number of allocation strategies for EV charging/discharging with different objectives have been reported in the literature [6], [8]–[11], [13], [15], [17]. We refer the interested reader to [2] for a comprehensive survey on EV charging scheduling and its challenges.

In scenarios where the EV-related specifics, including EV battery degradation factors, are known in advance, the problem of minimizing the overall cost in cooperative EV charging scheduling at smart CSs was investigated in [8]. Due to the unpredictable EV departure times, a closed-form solution was derived in [11] for the optimal charging power of an individual EV under the time-of-use (ToU) pricing model. Similarly, the authors in [6] proposed a performance-guaranteed online algorithm to achieve sub-optimal charging scheduling solutions which result in slightly higher costs compared to the optimal counterpart. In [13], the bidirectional V2G operation in a distributed network of CSs with the objective of providing frequency and regulation support to the power grid and reducing EV charging costs was addressed. In smart home applications, EVs can be integrated into home appliances in order to reduce the electricity costs of consumers. In this regard, the minimization of overall household electricity payment through participation in the demand response (DR) program integrated with EV scheduling was studied in [15].

In energy distribution systems, the interplay between various non-deterministic factors complicate the design of efficient scheduling mechanisms under uncertainty [20]–[22]. Particularly in V2G systems, the EV fleet size, the time intervals in which they request for charging/discharging services, and the percentage of V2G penetration are the main sources of uncertainty. To this end, research efforts have tackled uncertainty using approaches such as point estimate method [21] and hybrid possibilities-probabilities [20]. Along with several stochastic parameters, another critical factor that impacts the profits made by EV owners is the degradation/fluctuation costs associated with EV batteries. As detailed in [20] and [21], EV battery degradation accounts for both calendar degradation, which depends not only on the state of charge (SOC), but also on the battery temperature, and cycle degradation. Battery cycle degradation depends on the depth of discharge (DoD) and charging/discharging rates.

Another stochastic parameter that directly affects the participation in DR programs is the price of electricity during different times of the day. In [23], the authors investigated the impact of different pricing models on the energy consumption pattern of consumers in a price-based DR program for residential microgrids. Among different pricing models, the real-time pricing (RTP) strategy, where the electricity price is impacted by instantaneous EV charging/discharging patterns, has been widely adopted in V2G systems [10], [24]. Alongside this parameter, advanced optimization approaches are required to handle the underlying constraints in scheduling of EVs. The proposed algorithms should accommodate the complex set of system variables (EV fleet size and battery) as well as uncertainty in the energy demand.

A partial augmented Lagrangian optimization approach was proposed in [4] to cope with the coupling constraints among EVs in a distribution network. The convergence of the proposed algorithm to the global optimal was analyzed and its performance was studied under the IEEE 13-node distribution test network with heterogeneous EVs. In [14], a two-stage scheduling mechanism was proposed for large-scale scheduling of EVs with the objective of reducing the negative impact of their charging loads on the power grid. In the first stage, the EV charging/discharging plan is determined to minimize costs and the deviation of load curve on the grid while, the EV load management is considered in the second stage to follow the guiding load curve. Mixed optimization formulations are the most common mathematical tools which can effectively capture the complex set of constraints in EV scheduling optimization problems [10], [25], [26]. Due to the stochastic nature of variables as well as the intractability of mixed optimization problems, the greedy approach has been recognized as the most efficient method to obtain the near-optimal scheduling solutions within a reasonably short time period in online scheduling scenarios where information on EVs is unavailable beforehand [10], [27].

With regard to V2G system scalability, the authors in [12] studied the cost minimization problem of scheduling EV charging at multiple CSs where aggregators at different CSs co-ordinate with each other in energy trading. The problem of optimal interval allocation for charging/discharging EVs at homes and common parking lots for smart households prosumers was addressed in [10]. In their proposed model, majority of the EV population charged from the power grid when at homes during the night, while they mainly participate in discharging at office parking lots during day time. Additionally, recent technological advancements have facilitated the emergence of more sophisticated solutions for scalable V2G systems [1], [16]–[19]. Luo *et al.* [16] introduced the role of cloud computing infrastructures in grid energy and addressed some related challenges. The utilization of cloud computing for efficient EV scheduling has been scrutinized in [17]. For smart cities, the authors in [1] investigated the power generation and management in EV power supply equipment (D-EVSE) and proposed two algorithms to maximize the driver satisfaction in terms of service waiting time and to minimize D-EVSE stress level.

In spite of all the solutions available, scheduling of a large fleet of EVs in smart energy distribution systems where EV drivers have the flexibility in charging/discharging at different stations managed by individual aggregators has not been well explored. Furthermore, most of the existing efforts tend to maximize EV driver satisfaction or their profits, while neglecting the social welfare of the whole distribution system.

In this paper, we focus on how the weighted profit maximization impacts the obtainable profit for each EV and CS entity in a smart energy distribution system, where aggregators purchase required energy from the grid without the need for coordination among them. Considering the realistic costs for EV batteries, maintenance, and labor, we also obtain the optimal points on some noticeable parameters under such a setting. That is to say, we formulate the problem of social welfare maximization for V2G scheduling in a large-scale smart energy distribution system as an MINLP optimization problem. As a widely used approach to obtain efficient solutions with fast computational performance, we then present an online two-step greedy-based algorithm to solve the intractable optimization problem. Considering the best-case performance, simulation results verify that, compared to an alternative scheduling solution, our proposed algorithm improves the system social welfare by about 30% on average and the flatness of final grid electricity load by about 20% on average. The results further show the existence of optimal CS deployment and V2G penetration in the distribution system which can indeed be insightful when designing distributed V2G systems in smart cities.

III. SYSTEM MODEL DESCRIPTION

We consider a smart energy distribution system comprising of K spatially-distributed CSs at a large geographical scale in a smart city scenario. The energy trade between the CSs and the power grid provisioned by individual aggregators and under the control of smart meters is shown in Fig. 1. The distribution system operator (DSO) manages the operations of all aggregators in interaction with the power grid.

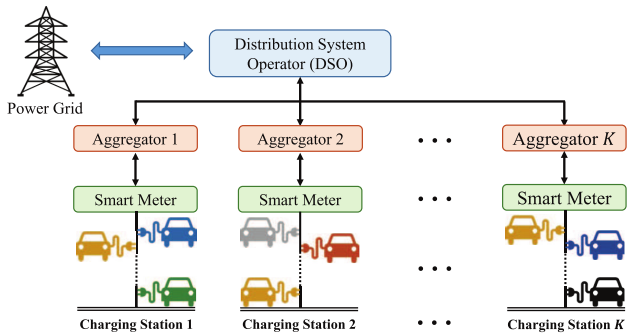

FIGURE 1. Bidirectional information/energy flow between the aggregators and power grid in a smart distribution system.

Although the aggregators are connected by a single DSO unit, they do not communicate or collaborate in energy or profit trading and work independently.

The EV set, represented by M, is defined as $M = M^{\mathrm{CG}} \cup M^{\mathrm{DG}} \cup M^{\mathrm{V2G}}$, where M^{CG} denotes the set of EVs that only have charging demands from the power grid, M^{DG} is the set of EVs that want to only discharge energy to the grid, and M^{V2G} is the set of EVs that participate in bidirectional V2G program. The vehicles participate in V2G or grid-to-vehicle (G2V) during their daily commute from home to work or vice versa. It is also assumed that the EVs in M^{DG} have sufficient energy for travelling to their destinations and are interested in returning some quantum of battery energy back to the grid or CS. The EVs participate in V2G operation in the course of their commute. Therefore, they do not move to CSs solely for the purpose of discharging and gaining profit [10].

The schedule for a single day is equally divided into $|T|$ discrete time slots, where each slot has the fixed duration of Δt time units [8], [28]. The EV arrival and departure time slots to and from charging station CS_k are denoted by $A_{a,k}$ and $D_{a,k}$, respectively. We assume non-preemptive charging/discharging scheduling of EVs at each CS in our system. The distance between EV a and CS_k at the time of departure from home and the constant electric motor force are denoted respectively, as $d_{a,k}$ and F. The battery capacity of EV a and its SOC at time slot t are given by B_a and B_a^t, respectively. Furthermore, the parameter $0 < r_a \leq 1$ is defined to control the final energy requirement of EV a based on its battery capacity. The initial energy stored in the battery of EV a at the time of departure from home and the final energy requirement are denoted by E_a^{init} and E_a^{fin}, respectively. The amount of energy consumed dwhile commuting from home to the CS is calculated as $F{\cdot}d_{a,k}$. Also, the maximum number of EVs that can be accommodated at CS_k is given by C_k^{max} and the binary decision variable $x_{a,k}^t$ indicates the allocation of EV a to CS_k at time slot t. With the maximum charging and discharging powers of P_c^{max} and P_d^{max} in each time slot, the amount of allocated charging/discharging power to EV a in CS_k at time slot t is indicated by real decision variable $e_{a,k}^t$.

The service interval of EV a at CS_k, i.e. the set of consecutive time slots for its charging/discharging operation, is denoted by $T_{a,k}$ with the first and last time slots given as $t_{a,k}^f$ and $t_{a,k}^l$, respectively. Each EV pays the maintenance cost (MC_k) to the CS while on the other side, the CS should pay the service cost (LC_k) to the labor in order to perform the maintenance. Due to high charging/discharging frequencies, our system also takes into account the degradation (η_1) and fluctuations (η_2) parameters which correspond to the auxiliary costs associated with the EV battery [10]. For convenience, the system notations and their descriptions are summarized in Table 1.

TABLE 1. System notations and descriptions.

Notation	Description
K	Number of CSs.
$M = \bigcup_X M^X$, $X \in \{\mathrm{CG}, \mathrm{DG}, \mathrm{V2G}\}$	Set of EVs with only charging (M^{CG}), only discharging (M^{DG}) or both (M^{V2G}) demands.
C_k^{max}	Maximum number of EVs that can be accommodated at CS_k.
$d_{a,k}$, F_a	Distance of EV a from home to CS_k and its electric motor force.
$\mathrm{MC}_k/\mathrm{LC}_k$	Maintenance/labor cost at each slot in CS_k.
Δt	Fixed time slot duration.
$A_{a,k}/D_{a,k}$	Times of arrival and departure of EV a at CS_k.
$T_{a,k} = \{t_{a,k}^f, t_{a,k}^{f+1}, \ldots, t_{a,k}^l\}$	Service interval of EV a at CS_k.
$S_{a,k}^t$	Consecutive slots before time slot t in charging/discharging period of EV a at CS_k.
N_k^t	Number of plugged-in EVs in slot t at CS_k.
P_c^{max}/P_d^{max}	Maximum EVs charging/discharging power at each time slot.
η_1, η_2, δ	Battery degradation, fluctuation, and weighting profit control parameters.
d_b, η_c	Battery self-discharge rate, battery charging efficiency (between 0 and 1).
E_a^{init}/E_a^{fin}	Initial/final battery energy of EV a.
B_a, B_a^t	Battery size of EV a and its SOC at time slot t.
r_a, $(0 < r_a \leq 1)$	Final fractional energy control parameter.
L_k^t, z_k^t	Non-EV electricity base load and overall load in time slot t at CS_k.
c_0^k, c_1^k c_2^k, c_3^k	RTP coefficients at bus of CS_k. Range and incremental price of energy-buyback step function model at CS_k.
ω, γ	Fitting parameters in EV battery calendar degradation model.
θ_a	Temperature (in degrees) of battery EV a.
α_1, α_2, α_3	Fitting parameters in battery cycle degradation model related to DoD.
β_1, β_2, β_3, β_4	Fitting parameters in battery cycle degradation model related to charging/discharging rate.
$x_{a,k}^t$, $e_{a,k}^t$	Binary variable for EV a allocation to CS_k and its power at time slot t.

A. COMMUNICATION SYSTEM

As shown in Fig. 1, each CS is managed by a single aggregator that establishes the information and energy interactions between the power grid and EVs under the control of a smart meter. It is assumed that each aggregator purchases the required energy from the power grid and hence, no coordination between the aggregators is required.

However, the price of purchase depends on the CS location. EVs request for charging/discharging services when they commute between home and work such that the time slots at which they arrive at CSs are distributed over the scheduling day. Before CS selection, the EV transmits a message containing data such as its distance to CSs, arrival/departure at each CS, initial/final energy requirements, and battery capacity to all aggregators. The communication between EVs and the aggregators is established via cellular (LTE, 4G/5G) wireless communication based on the V2G network infrastructure in place [18], [19]. Depending on the demand load and electricity price at each CS, the associated aggregator then computes the achievable profit if the EV is allocated to its CS and sends this information back to the EV. Therefore, there is no need for directly transmitting the demand load or the electricity price to the EV and only the achievable profit is communicated with the EV. Upon receiving information on the achievable profit from all K aggregators, the EV then subscribes to the most profitable CS for energy trading.

B. ELECTRICITY PRICING MODEL

In smart EV scheduling, the instantaneous electricity price is directly affected the charging/discharging power of EVs at each time instant. Among the different pricing strategies, the RTP schema has been well-accepted wherein the instantaneous price is determined based on overall electricity load at each time slot [8], [28]. In the proposed distribution system, we utilize the RTP model in which the time-dependent price, $p(k,t)$, is in linear relation with the load at that time slot, i.e. $p(k,t) = c_0^k + c_1^k z_k^t$ for $z_k^t \geq 0$, where c_0^k and c_1^k are non-negative real numbers indicating the intercept (in $\$/kWh$) and slope (in $\$/kWh/kW$), respectively, of the RTP model at the bus to which CS_k is connected. The load on CS_k at time slot t, denoted by z_k^t, is expressed in terms of the base load generated at CS_k by non-EV demands (L_k^t) as follows:

$$z_k^t = L_k^t + \sum_{a \in M} x_{a,k}^t \cdot e_{a,k}^t\,, \quad 1 \leq k \leq K; 1 \leq t \leq |T|\,. \tag{1}$$

Our system also considers the energy-buyback step function pricing model for when the electricity load on the grid becomes negative due to high discharging load from the EVs. Using step function pricing for the negative load motivates the EVs to return back the surplus battery energy to the grid (for preserving in the energy storage systems (ESSs)) while paid less compared to the case when there is high demand on the grid. Denoting c_2^k and c_3^k as the range (in kW) and the incremental price (in $\$/kWh$) of the step function model at the bus to which CS_k is connected, respectively, the electricity price at load $z_k^t < 0$ is given by $p(k,t) = c_0^k + \lceil |z_k^t|/c_2^k \rceil \cdot c_3^k$.

C. PROFIT COMPUTATION

In a distribution system, the social welfare is composed of the weighted summation of profits obtained by both, EVs and CSs participating in energy trading. The profit that each side makes depends on its revenue and the associated costs [23]. On the EV side, the overall profit made by EV owners during time slot t at CS_k, denoted by $P_{EV}(k,t)$, is computed as the total revenue from charging/discharging minus the maintenance and battery degradation/fluctuation costs. The EV fleet revenue at time slot t is given by [23], [28]:

$$R_{Fleet}(k,t) = -\int_{L_k^t}^{z_k^t} p(k,\tau)\, dz_k^\tau\,. \tag{2}$$

As mentioned earlier, $p(k,\tau)$ follows the linear pricing model as long as the load on power grid is positive and follows the energy-buyback step model when the grid bears negative load. The negative sign in (2) is to confirm the fact that EV owners get negative/positive revenue from charging/discharging operations. In practice, the two major auxiliary costs associated with EV charging/discharging operation are the battery fluctuation/degradation [8], [28] due to high charging/discharging powers and the EV maintenance cost at the station. Therefore, the auxiliary cost of EV a at time slot t in CS_k is derived as the summation:

$$C_{Fleet}(k,t) = \sum_{a \in M} x_{a,k}^t \cdot \left(\text{MC}_k + \eta_1 \cdot \text{DC}_{a,k}^t + \eta_2 \cdot \text{FC}_{a,k}^t\right). \tag{3}$$

The degradation of EV battery depends on factors such as the charging/discharging rate, environmental temperature, and the battery DoD which negatively impact the battery efficiency over the long time horizon [21]. Mathematically speaking, the battery degradation cost $\text{DC}_{a,k}^t$ is computed as the summation of calendar and cycle degradation costs [21]:

$$\text{DC}_{a,k}^t = \text{DC}_{a,k}^{CAL_t} + \text{DC}_{a,k}^{CYC_t}\,, \tag{4}$$

and the battery fluctuation cost is obtained as follows:

$$\text{FC}_{a,k}^t = \left(e_{a,k}^t - e_{a,k}^{t-1}\right)^2. \tag{5}$$

The battery calendar degradation cost of EV a in CS_k at time slot t is computed using the following expression [21]:

$$\text{DC}_{a,k}^{CAL_t} = B_a \cdot e^{B_a^t/\omega} \cdot e^{\theta_a/\gamma} \cdot \sqrt{\Delta t}\,, \tag{6}$$

where ω and γ are the fitting parameters for battery calendar degradation, while θ_a is the constant temperature (in degrees) of battery EV a. B_a^t represents the battery SOC at time slot t which follows the relation given below, where the battery self-discharge rate d_b and charging efficiency η_c (between zero and one) are set to respectively, 0 and 1 [28]:

$$B_a^t = (1 - d_b) B_a^{t-1} + \eta_c \cdot \Delta t \cdot e_{a,k}^t. \tag{7}$$

In other words, the battery SOC at time slot t in our model is simply based on the SOC at time slot $t-1$ and the charging or discharging power at time slot t. Also, the battery cycle degradation cost can be expressed as follows [21]:

$$\begin{aligned}\text{DC}_{a,k}^{CYC_t} = &\left(\alpha_1 (B_a - B_a^t)^2 + \alpha_2 (B_a - B_a^t) + \alpha_3\right) \\ &\cdot \left(\beta_1 |e_{a,k}^t|^3 + \beta_2 |e_{a,k}^t|^2 + \beta_3 |e_{a,k}^t| + \beta_4\right),\end{aligned} \tag{8}$$

where the coefficients α_1, α_2, and α_3 are the fitting parameters of battery cycle degradation related to DoD, while the

coefficients β_1, β_2, β_3, and β_4 are the fitting parameters of battery cycle degradation related to charging/discharging rate of EV at time slot t. Note that the parametric values for both calendar and cycle degradation models are obtained using the experimental plots in [29] for simulation.

From (2) and (3), we now calculate the overall profit (Φ) of EVs at CS_k during time slot t as below:

$$\Phi_{Fleet}(k,t) = R_{Fleet}(k,t) - C_{Fleet}(k,t). \tag{9}$$

For the CSs, the profit gained from charging/discharging of EVs follows the same relation as (9), where the revenue of CSs is the negative of (2) and the associated cost is given by:

$$C_{CS}(k,t) = \sum_{a\in M} x_{a,k}^{t} \cdot \left(\mathrm{LC}_k - \mathrm{MC}_k\right). \tag{10}$$

It should be noted that the revenue that CSs gain is only from charging/discharging of EVs; therefore, the revenue of CSs is the negative sign of EVs revenue (as given in (2)). It is also noteworthy to mention that in (10), the net cost of CS including the payment to labors and income from EV drivers (paid for maintenance) is taken into consideration.

As the aim of the proposed framework is to maximize the social welfare of the system, i.e. the overall profit of both EVs and CS entities, an adjustable control parameter $0 \le \delta \le 1$ is introduced, such that the maximum profit is achieved for EVs with $\delta = 0$, while the CSs achieve the maximum profit when $\delta = 1$. Hence, the overall profit during $|T|$ time slots is calculated as:

$$\Phi_{tot} = (1-\delta)\sum_{k=1}^{K}\sum_{t=1}^{|T|}\Phi_{Fleet}(k,t) + \delta\sum_{k=1}^{K}\sum_{t=1}^{|T|}\Phi_{CS}(k,t). \tag{11}$$

In practical terms, the weighting parameter δ is determined by the CS aggregators depending on the EV arrival pattern and the profit interests of both sides of the deal. In situations when there are more EV arrivals for charging/discharging at certain CSs, the corresponding aggregators determine δ such that it reduces the profit obtained by EVs to the extent where the maximum system social welfare is achieved. In contrast, with lesser EVs arriving at a CS, the aggregator decides on the δ value that favors the EVs in gaining profit.

IV. SOCIAL WELFARE MAXIMIZATION PROBLEM

From the network operation point of view, it is important to achieve scheduling solutions that maximize shared benefits of both participating sides in the energy distribution system. Following this principle, the objective of our system model is to schedule the allocation of EVs to CSs so as to achieve the maximum shared profits for both, EVs and CSs. In this section, we define the social welfare maximization problem for EV charging/discharging scheduling in an offline manner where all information about the EVs are known in advance. As stated before, mixed optimization models are the most efficient tools that can capture the system behavior involving different types of decision variables and constraints. Thus, for all $a \in M$, $1 \le k \ne k' \le K$, $t \in T_{a,k}$, $t' \in T_{a,k'}$, and $1 \le t \le |T|$, the problem is formulated as the following MINLP optimization model:

$$\text{Maximize} \quad \Phi_{tot} \tag{12}$$

subject to:

$$x_{a,k}^{t} = 0, \qquad t \in \left[1, t_{a,k}^{f} - 1\right] \bigcup \left[t_{a,k}^{1} + 1, |T|\right], \tag{13}$$

$$\sum_{k=1}^{K}\sum_{t=t_{a,k}^{f}}^{t_{a,k}^{1}} x_{a,k}^{t} \ge 1, \tag{14}$$

$$\prod_{t,t'} x_{a,k}^{t} \cdot x_{a,k}^{t'} = 0, \tag{15}$$

$$\sum_{t\in T_{a,k}} x_{a,k}^{t} = \left(\prod_{t\in T_{a,k}} x_{a,k}^{t}\right) \cdot |T_{a,k}|, \tag{16}$$

$$\sum_{a\in M} x_{a,k}^{t} \le C_k^{max}, \tag{17}$$

$$z_k^t = L_k^t + \sum_{a\in M} x_{a,k}^{t} \cdot e_{a,k}^{t}, \tag{18}$$

$$0 \le E_a^{init} - d_{a,k}\cdot F_a + \sum_{t'\in S_{a,k}^{t}} x_{a,k}^{\prime} \cdot e_{a,k}^{t'} \le B_a, \tag{19}$$

$$E_a^{fin} = E_a^{init} - d_{a,k}\cdot F_a + \sum_{k=1}^{K}\sum_{t\in T_{a,k}} x_{a,k}^{t}\cdot e_{a,k}^{t} = r_a \cdot B_a, \tag{20}$$

$$0 \le e_{a,k}^{t} \le P_c^{max}, \qquad a \in M^{\mathrm{CG}}, \tag{21}$$

$$-P_d^{max} \le e_{a,k}^{t} \le 0, \qquad a \in M^{\mathrm{DG}}, \tag{22}$$

$$-P_d^{max} \le e_{a,k}^{t} \le P_c^{max}, \qquad a \in M^{\mathrm{V2G}}. \tag{23}$$

The objective function (12) maximizes the overall joint profit of EVs and CSs given in (11). The equality constraint (13) ensures that every EV is allocated to a CS only during the time slots within its charging/discharging interval at that CS. Constraints (14)-(16) guarantee the non-preemptive allocation of EVs to only one CS, and (17) enforces an upper bound on the number of EVs that can plug-in to a CS at every time slot. Also, (18) states the instantaneous electricity load at each CS and (19) ensures that the EV battery energy level during its charging/discharging interval (considering the initial energy at the time of departure from home and the consumed energy from home to CS) is non-negative and below its battery capacity. Equation (20) guarantees that the final energy stored in the EV battery matches with the initial demand determined by EV driver. Finally, depending on the vehicle type, (21)-(23) specify the lower and upper charging/discharging power bounds in each slot.

In spite of some similarities with the EV battery-associated costs reported in [18], [24], [28], it should be noted that the proposed optimization problem significantly differs in the following aspects. First, our objective function aims to maximize the weighted social welfare from charging/discharging of EVs in energy distribution system, while the model in [24]

minimizes the operational costs of CSs integrated with ESSs. Similarly, the other models either minimize the overall costs of wind power imbalances and EV-related expenses in energy purchase [28] or only maximize the profit of EVs [18]. Moreover, our system model considers the charging/discharging of on-move EVs in a geographically large-scale which, unlike the above models, accounts for the EV energy consumption during traveled distances, the CS capacity, the EV service costs, and the battery energy level constraints.

V. ONLINE GREEDY-BASED ALGORITHM

The maximization problem in (12)-(23) belongs to the class of intractable problems since the allocation of EVs to CSs are integer variables. Besides, the non-convexity of the problem limits the use of standard solutions for convex optimization problems. Linear programming (LP) relaxation combined with BB can be leveraged to find the optimal solutions to the offline problem formulation [25]. The challenge in using BB, however, lies in the significant computation complexity incurred, specially when the size of the problem including the number of time slots, the number of CSs or the number of EVs increases. As another challenge faced in real-time implementation, the information on future EV requests are not accessible in advance which makes BB an infeasible solution. To overcome such practical issues, we design an effective online and distributed greedy-based algorithm with low computational complexity, named *Greedy Multiple Charging Stations* (**GreedyMCS**), given in Algorithm 1.

Algorithm 1 GreedyMCS

Input: $Data(a,k) \triangleq (A_{a,k}, D_{a,k}, T_{a,k}, E_a^{init}, B_a, E_a^{fin}, r_a)$ for EV $a \in M$ and CS $k \in K$, and parameter δ.
Output: Assignment of EV a to candidate CS.

while vehicle $a \in M$ requests for service **do**
  Broadcast message with $Data(a,k)$ to all CSs.
  for each CS_k, $1 \le k \le K$ **do**
    if $\forall t \in [A_{a,k}, D_{a,k}], N_k^t + 1 \le C_k^{max}$ **then**
      if $a \in M^{CG}$ **then**
        Run ComputeProfit_Charging(a,k).
      else if $a \in M^{DG}$ **then**
        Run ComputeProfit_Discharging(a,k).
      else
        Run ComputeProfit_V2G(a,k).
      end if
    end if
  end for
  Send back message containing $\phi_{EV}(a,k)$ and $\phi_{CS}(a,k)$ from each aggregator to vehicle a.
  Transmit reservation message to $CS_{k'}$, where $k' = arg_k \ max\{(1-\delta)\phi_{EV}(a,k) + \delta\phi_{CS}(a,k)\}$.
  $N_{k'}^t = N_{k'}^t + 1, \ \forall t \in [A_{a,k'}, D_{a,k'}]$
  Solve NLP problem (24) to find the optimal service plan for EV a at $CS_{k'}$.
end while

The key idea is that instead of solving the complex MINLP problem, Algorithm 1 initially solves the integer optimization part of the problem by selecting the most suitable CS using a greedy-based heuristic. After CS selection, the algorithm then determines the amount of energy to be traded at each time slot between the EV and power grid in the selected CS by solving a local optimization problem using standard optimization solver. It is noteworthy to mention that after resolving the integer part of the problem (i.e. CS selection), the problem is converted to NLP and hence, solving it using standard solver does not incur high complexity. Also note that our solution also accounts for the uncertainty in system parameters similar to techniques given in [20]. In what follows, we discuss each phase of the proposed algorithm.

A. CS SELECTION STRATEGY

Once a charging/discharging service is requested by EV a, its contextual data is transmitted to all aggregators wirelessly. Each aggregator then runs a local heuristic depending on the EV type to regulate its charging/discharging plan as well as the local profit obtainable at that CS. Algorithm 2 shows the pseudocode for the heuristic, referred to as **ComputeProfit_Charging**, which deals only with the charging demands. The partial revenue that EV a obtains from charging/discharging at CS_k in time slot $t \in T_{a,k}$ is achieved by integrating the price relation over the electricity load which changes from the current z_k^t to the accumulated load $z_k^t + e_{a,k}^t$. Considering the auxiliary costs of maintenance and battery degradation/fluctuation over the entire service interval of EV a, its achievable profit is then calculated similar to equation (9). The partial profit of CS_k obtained by allocating EV a is also computed in a similar manner. Note that functions Φ_{Fleet} and Φ_{CS} in the problem formulation which take the CS and time instant as input arguments returns the obtainable profit when a fleet of EVs are allocated to a CS at a given time slot. Nonetheless, in the online implementation of the algorithm, the functions ϕ_{EV} and ϕ_{CS} which take the EV and CS as input arguments return the obtainable profits when a particular EV is allocated to a given CS.

The subroutine for computing the profit at each CS employs an updating heuristic to determine the charging/discharging plan for the EV. Subject to the EV participation, the local schedulers execute the related profit computation subroutine in order to determine the local profit that the EV and CSs obtain considering the instantaneous electricity price and the EV contextual data such as its arrival/departure times, battery capacity, and initial/final energy demands. Firstly, the average electricity price in all time slots during the charging/discharging interval of the EV is computed. The energy demand is subsequently divided equally among all time slots of the interval (lines 2-4). For the number of iterations equal to the interval length (line 5), the power of the EV is upgraded in each time slot proportional to the gap between average and current prices (lines 6-7). The charging/discharging power in the remaining slots is then updated to satisfy both (19) and (20) (lines 8-22).

Algorithm 2 ComputeProfit_Charging(a, k)

if $\forall t \in [A_{a,k}, D_{a,k}], N_k^t + 1 \leq C_k^{max}$ **then**
  for $t = t_{a,k}^f$ to $t_{a,k}^l$ **do**
    $e_{a,k}^t \leftarrow (E_a^{fin} - E_a^{init})/|T_{a,k}|$.
  end for
  for $t' = t_{a,k}^f$ to $t_{a,k}^l - 1$ **do**
    $avgPrice \leftarrow \sum_{t \in T_{a,k}} p(k,t)/|T_{a,k}|$.
    $e_{a,k}^{t'} \leftarrow \frac{\left(2 \cdot avgPrice - p(k,t')\right) \cdot e_{a,k}^{t'}}{avgPrice}$.
    if $e_{a,k}^{t'} > P_c^{max}$ **then**
      $e_{a,k}^{t'} \leftarrow P_c^{max}$.
    end if
    if $e_{a,k}^{t'} < 0$ **then**
      $e_{a,k}^{t'} \leftarrow 0$.
    end if
    $totalCharge \leftarrow \sum_{t=t_{a,k}^f}^{t'} e_{a,k}^t$.
    $avgCharge \leftarrow \frac{E_a^{fin} - E_a^{init} - totalCharge}{|T_{a,k}| - t'}$.
    if $avgCharge > P_c^{max}$ **then**
      $\Delta e \leftarrow \frac{(t_{a,k}^l - t')(avgCharge - P_c^{max})}{t' - t_{a,k}^f}$.
      $avgCharge \leftarrow P_c^{max}$.
    else if $avgCharge < 0$ **then**
      $\Delta e \leftarrow -\frac{(t_{a,k}^l - t')avgCharge}{t' - t_{a,k}^f}$.
      $avgCharge \leftarrow 0$.
    end if
    $e_{a,k}^t \leftarrow e_{a,k}^t + \Delta e, \ \forall t \in [t_{a,k}^f, t']$.
    $e_{a,k}^t \leftarrow avgCharge, \ \forall t \in [t' + 1, t_{a,k}^l]$.
    Update z_k^t with $e_{a,k}^t, \ \forall t \in [t_{a,k}^f, t_{a,k}^f]$.
    $p(k,t) \leftarrow c_0 + c_1 z_k^t, \ \forall t \in [t_{a,k}^f, t_{a,k}^f]$.
  end for
  Compute $\phi_{EV}(a,k)$ and $\phi_{CS}(a,k)$.
end if
return $\phi_{EV}(a,k)$ and $\phi_{CS}(a,k)$.

In consonance with (1), the electricity load on the grid is then updated and eventually, the procedure returns the local obtainable profits.

Similar heuristics are executed for cases when EVs participate in discharging (**ComputeProfit_Discharging**) and V2G (**ComputeProfit_V2G**) operations. In the case of discharging, the only difference is that the discharging load of the EV is distributed over the entire time interval such that larger discharging power is assigned to time slots with higher electricity load on the grid and vice versa. On the other hand, for EVs participating in V2G, the charging and discharging powers assigned to time slots with, respectively, low and high grid electricity loads are adjusted based on the difference between the current and average load on the power grid.

Depending on the EV type, a reply message containing the computed profit achievable by the EV is sent by all CS aggregators. As stated in Algorithm 1, upon receiving the reply message, the EV compares the profits to decide on the most appropriate CS that yields the highest social welfare. The EV then responds to the target CS with a reservation message indicating its willingness for service at that station.

It should be noted that in the **GreedyMCS** algorithm, solving the optimization problem using the heuristics is performed in a distributed manner at local aggregators and finding the most suitable CS is performed at the EV side. Although a centralized solution integrates the computational operations in a single point and simplifies the intercommunication burden, the methodologies which rely on running huge computational tasks in a centralized way suffer from low reliability due to the single point of failure and also high computational complexity. Since the comparison operation to find the most suitable CS is light-weighted compared to running the heuristics at the aggregators, the **GreedyMCS** algorithm is a decentralized approach and thus, easily scalable to large-scale V2G systems.

B. POWER CHARGE/DISCHARGE AT TARGET CS

When EV a is plugged-in to the target station $\text{CS}_{k'}$, the energy traded between the power grid and the EV is handled by the aggregator which finds the optimal solution to the following local optimizer based on root mean square deviation (rmsd):

$$\text{Maximize} \quad \sqrt{\frac{\sum_{t \in T_{a,k'}} (z_{k'}^t + e_{a,k'}^t - \bar{z}_{k'})^2}{|T_{a,k'}|}}, \tag{24}$$

with constraints (19)-(23) by replacing station index k' in the equations. In the objective function (24), $\bar{z}_{k'}$ is the average load over all time slots at $\text{CS}_{k'}$. The aggregator of target station interacts with power grid for energy exchange which is regulated and monitored by the smart meter at that station.

C. COMPLEXITY ANALYSIS

According to Algorithm 1, each EV sends its data to all CSs in $O(1)$ time. Once the profit is computed locally at all CSs, the aggregators respond with the calculated profit resulting in message complexity of $O(1)$. That is to say, with $|M|$ vehicles and K CSs in the distribution system, the message complexity of GreedyMCS is $O(|M| \cdot K)$ in the worst case.

The total computational time of the algorithm includes the time for computing the profit at CSs and the search time for the maximum profit made by the EV locally. Since the CSs compute the profit independent of each other, we investigate the profit computation time taken by a single CS. In the worst case, the charging/discharging interval of the EV covers the entire scheduling day including $|T|$ time slots. Inclusive of time spent on selecting the most profitable station as well as the time for solving the local optimization problem (24), denoted by t_{opt}, it is observed that the worst case time complexity of **GreedyMCS** is of order $O\big(|M| \cdot (|T|^2 + K + t_{opt})\big)$. We once again highlight that after the CS selection phase, the problem is converted to NLP and solving it using standard solver at the target CS does not incur high complexity.

D. REMARKS ON OPTIMALITY

Recall that the formulated social welfare maximization problem belongs to the class of intractable problems. It has been shown that reducing the search space of mixed optimization problems using an efficient heuristic provides some guidelines to judge the optimality gap of such problems [30]. In this work, we exploit the **GreedyMCS** algorithm to reduce the original MINLP problem to a tractable NLP problem and then solve it using a standard optimization solver. We expect the gap between the solution returned by **GreedyMCS** and the optimal solution obtained by directly solving the original MINLP problem to be small. This is due to the fact that using a sub-optimal heuristic to determine the energy trade between EV at a selected CS and the power grid yields much degraded performance compared to finding the optimal CS for the EV using a heuristic. Since our algorithm solves the CS selection part using a heuristic and the amount of traded energy is decided using the standard solver, we expect a small gap with respect to the optimal MINLP solutions. Verifying this fact for small instances of the problem is an interesting direction which we consider as future work. It is also worth mentioning that although the proposed algorithm is sub-optimal, it finds the solutions to the problem (12)-(23) with a reasonably low computational complexity.

VI. SIMULATION RESULTS

In this section, we evaluate the performance of **GreedyMCS** through simulations in terms of social welfare of the system, the obtainable profits for each participant in the system (EVs and CSs, and the ancillary services provided to the power grid. For comparison purpose, we adopt the *Random Multiple Charging Stations* (**RandomMCS**) [31] approach as the best baseline solution . In **RandomMCS**, each time an EV requests for charging/discharging service, it is randomly assigned to a CS that does not violate its service demand. We further evaluate the system performance considering the uncertainty in system parameters by utilizing the possibilities-probabilities approach given in [20]. Particularly, we investigate the impact of parameters such as the number of EVs, different EV departure times, the number of CSs, and the V2G penetration probability on the system performance and provide some insights on the obtained results. The algorithms are implemented in MATLAB and the CVX solver package [32] is used to solve the local rmsd-based optimization at each CS. It is noteworthy to mention that all the data for EVs and CSs used in the simulations are generated by programs written in MATLAB and are described in the following sub-section.

A. SIMULATION SET-UP

A single V2G scheduling day is considered, which is divided into $|T| = 24$ equal time slots with $\Delta t = 1$ hour. In our setting, 1000 EVs depart from homes towards offices in the morning at random times taken from the uniform interval U[5 a.m., 12 p.m.]. The maximum number of EVs accommodated in each CS at each time slot is chosen from the uniform interval $U[105, 110]$. Also, 10 CSs are located on a 4.8 kV distribution network (IEEE 37 bus) shown in Fig. 2. The CS locations are identified with the help of OpenDSS and are optimal in terms of minimal power loss and required voltage profile (0.93 p.u. to 1.03 p.u.) under maximum loading condition at each station during the system peak. Unless otherwise stated, it is assumed that 50% of EVs participate in V2G, while the remaining equally engage in charging/discharging operations. The distance from home to CS_k ($d_{a,k}$) for EV a is chosen from the uniform interval [2 km, 5 km], its average speed from the interval [50 km/h, 60 km/h], and the electric motor force from the interval U[3 kWh/km, 5 kWh/km] [10]. The time at which the EVs arrive at each CS varies depending on distance and their average speed.

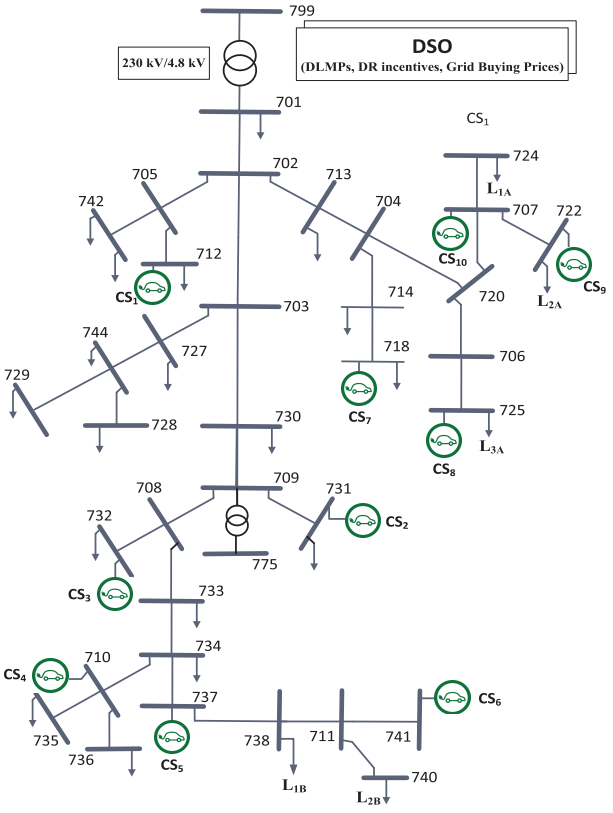

FIGURE 2. The IEEE 37 bus distribution system with 10 CSs.

Each EV decides on a desired time duration for service at each CS based on its future trip plan which, for simplicity, we suppose follows the uniform distribution U[3 h, 6 h]. The first and last time slots of charging/discharging interval for EV a at CS_k are determined by the CS operator with integer values from uniform intervals $U\big[\lceil A_{a,k}\rceil, \lceil A_{a,k}\rceil + \lfloor(\lfloor D_{a,k}\rfloor - \lceil A_{a,k}\rceil)/2\rfloor\big]$ and $U\big[\lfloor D_{a,k}\rfloor - \lceil(\lfloor D_{a,k}\rfloor - \lceil A_{a,k}\rceil)/2\rceil, D_{a,k}\big]$ [10]. The initial battery energy level of EV a at its departure time from home is chosen from the interval $U[0.7B_a, 0.9B_a]$, while the available battery energy upon its arrival to each CS is dependent on the distance travelled and its motor force.

For EVs with charging requests, the target energy determined by the driver falls within the uniform interval $U[0.7B_a, 0.9B_a]$ and for discharging, the battery energy level after discharging is taken from the interval $U[\min\{0.4B_a, E_a^{init} - d_{a,k} \cdot F_a\}, \min\{0.6B_a, E_a^{init} - d_{a,k} \cdot F_a\}]$. All EVs are assumed to have the ideal battery capacity of 100 kWh with maximum charging and discharging powers of 15 kW and 10 kW in each time slot, respectively. Hence, the maximum charging power coincides with the charging rate of $15/100 = 0.15$ C in [33].

The CS locations in IEEE 37 bus distribution network are chosen optimally to minimize the overall system loss and to maintain the voltage profile and line flows within the required limits. For this optimal study, we consider each CS to be capable of handling a maximum demand of 2 MW, i.e. more than 15 kW $\times$ 110, in each time slot when all plug-in chargers are in use. Considering the overall system peak load, this shows that the grid is capable of handling the maximum load imposed by EVs at CSs without violating the grid operational limits. Moreover, CSs not only handle V2G, but G2V as well, which alleviates the load on the system.

Li-ion battery-equipped EVs with temperature (θ) within range $U[-20°\text{C}, 60°\text{C}]$ [29] are considered in our simulations. Battery degradation/fluctuation coefficients are set to $\eta_1 = 10^{-3}$ \$/kWh^2 and $\eta_2 = 2 \times 10^{-3}$\$/kWh^2 following the simulation study in [10]. The fitting parameters for battery calendar and cycle degradation costs are taken from the experimental degradation plots reported in [29]. Solving the system of equations, we obtain the fitting values of $\omega = -3.8898$ and $\gamma = -6.9242$ for the calendar degradation cost in (6), and $\alpha_1 = 4.24 \times 10^{-8}$, $\alpha_2 = -4.42 \times 10^{-7}$, $\alpha_3 = 8.2 \times 10^{-6}$, $\beta_1 = -1.2$, $\beta_2 = 3.84$, $\beta_3 = -2.3$, and $\beta_4 = 0.66$ for cycle degradation cost in (8). The linear and step-function pricing model coefficients are selected from the uniform intervals $c_0^k \in U[10^{-3} - 0.0005$ \$/kWh, $10^{-3} + 0.0005$ \$/kWh], $c_1^k \in U[2 \times 10^{-3} - 0.0005$ \$/kWh/kW, $2 \times 10^{-3} + 0.0005$ \$/kWh/kW], $c_2^k \in U[5$ kW, 10 kW], and $c_3^k \in U[0.1$ \$/kWh, 0.3 \$/kWh] at all buses where the CSs are located. A typical daily base load forecast that fluctuates between 10 kW (low) and 70 kW (high) is also adopted at each CS [10]. An instance of the average base load at all 10 CSs over a summer day is shown in Fig. 3. We also assume that the EV maintenance and service costs have uniform distributions $U[\$\,0.3, \$\,0.5]$ and $U[\$\,0.2, \$\,0.4]$, respectively, in each time slot at every CS [10]. To evaluate the performance of **GreedyMCS** under such a setting, we need to initialize the set of deterministic variables used in the system and optimization problem (12)-(23). The initial values for the system variables used in the simulations are summarized in Table 2. The simulation results that follow have been averaged over 10 runs within 90% confidence interval.

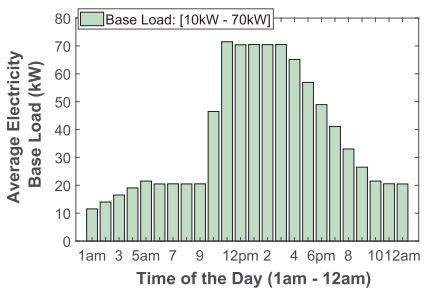

FIGURE 3. Typical base load profile for a single summer day.

TABLE 2. Simulation parameters and values.

Parameter	Value
Number of EVs	1000
Number of CSs (K)	10
Time slot duration (Δt)	1 hour
EV capacity of each CS in each time slot	$U[105, 110]$
Home departure time	$U[5$ a.m., 12 p.m.]
Distance to each CS	$U[2$ km, 5 km]
Average EV speed	$U[50$ km/h, 60 km/h]
EV electric motor force	$U[3$ kWh/km, 5 kWh/km]
EV battery capacity	100 kW
Battery initial/final energy level	$U[70\%, 90\%]$
Max. charging & discharging power per Δt	10 kWh, 15 kWh
EV charging rate	0.15 C
Battery degradation & fluctuation coefficients	$\eta_1 = 0.001$ \$/kWh^2, $\eta_2 = 0.002$ \$/kWh^2
Battery temperature	$U[-20°\text{C}, 60°\text{C}]$
Battery calender degradation parameters	$\omega = -3.8898$, $\gamma = -6.9242$
Battery cycle degradation parameters related to DoD	$\alpha_1 = 0.0424 \times 10^{-6}$, $\alpha_2 = -0.442 \times 10^{-6}$, $\alpha_3 = 8.2 \times 10^{-6}$
Battery cycle degradation parameters related to charging/discharging rate	$\beta_1 = -1.2$, $\beta_2 = 3.84$, $\beta_3 = -2.3$, $\beta_4 = 0.66$
Intercept of RTP model (c_0 in \$/kWh unit)	$U[0.0005, 0.0015]$
Slope of RTP model (c_1 in \$/kWh/kW unit)	$U[0.0015, 0.0025]$
Range of step price model (c_2 in kW unit)	$U[5, 10]$
Incremental of step model (c_3 in \$/kWh unit)	$U[0.1, 0.3]$
EV maintenance cost per Δt	$U[\$\,0.3, \$\,0.5]$
EV service cost per Δt	$U[\$\,0.2, \$\,0.4]$

B. ELECTRICITY PRICING AND EV DISTRIBUTION

The EV charging/discharging behavior in the energy distribution systems directly impacts the electricity price during different time intervals of the day. It is therefore, essential for V2G system designers to devise efficient scheduling mechanisms that adjust the time-dependent electricity price in a controlled manner. As our first simulation, we investigate the impact of EV charging/discharging on the instantaneous electricity price using our proposed algorithm.

Fig. 4 plots the mean electricity base load and EV charging/discharging power load at each Δt for all CSs during time interval [7 a.m., 6 p.m.]. It is evident from Fig. 4(a) that, on average, EVs demand for high charging power at time slots with low base load, while they return back the energy to the grid when the base load is high. In particular, stations

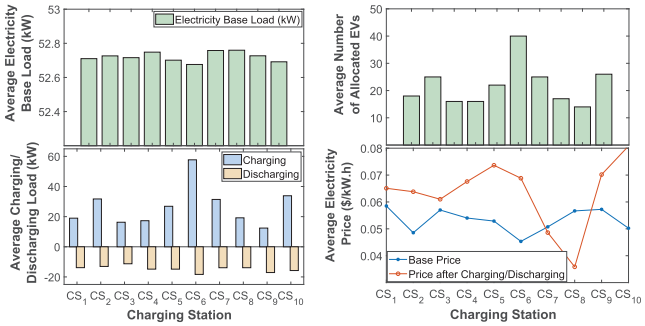

(a) (b)

FIGURE 4. **(a) Mean electricity base load and EV charging/discharging load (b) Average EV population and electricity price at each CS during time interval [7 a.m., 6 p.m.].**

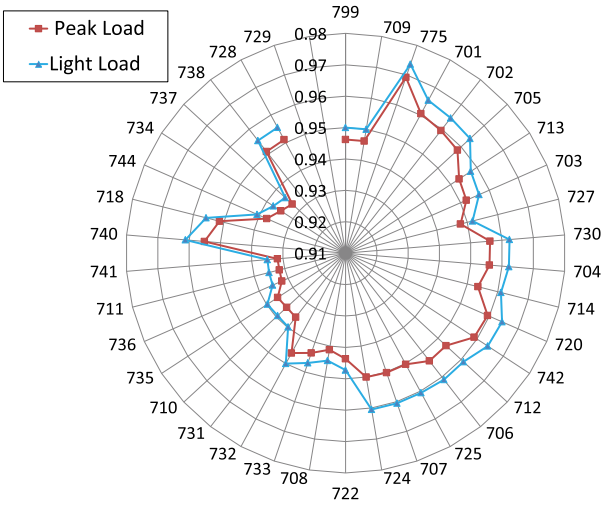

FIGURE 5. **Voltage profile of the system buses during peak and light load conditions.**

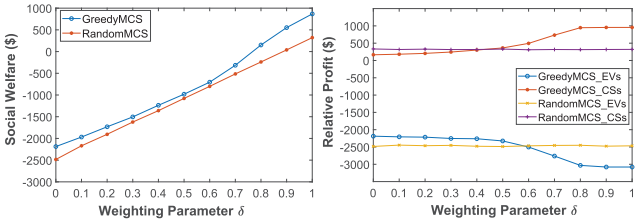

(a) Social welfare. (b) Relative profit.

FIGURE 6. **Comparison of GreedyMCS with RandomMCS in terms of (a) the overall social welfare and (b) the joint EVs and CSs profit for varying δ values.**

CS_6 and CS_{10} that have the lowest base loads receive more demands for EV charging as compared to the other stations. Similarly, the average charging load of CS_5 is higher than that of CS_3 and CS_4 due to its relatively lower base load. Although the base load at CS_2 is slightly higher than that at CS_1, it bears more charging load as higher number of EVs have been allocated to it due to some unexpected situations that will be explained in the subsequent section. Fig. 4(b) depicts the mean distribution of allocated EVs and real-time electricity price at each time slot for all CSs during the time interval [7 a.m., 6 p.m.]. As seen in this figure, the real-time electricity price fluctuates after charging/discharging at each CS in accordance with the number of plugged-in EVs at the stations. We also observe that the average electricity price after charging/discharging and the average EV charging load (Fig. 4(a)) exhibit very similar patterns. This reveals the dependency of real-time electricity pricing on the charging load of plugged-in EVs. Interestingly, though EVs have similar home departure times during the day, the reason why most EVs are allocated to CS_6, whereas the minimum to CS_8 is due to uncertainty in EV arrivals and distance to the CSs.

Fig. 5 shows the voltage profile of the system buses during peak and light EV load periods for one day. During simulation, the other loads on the system followed the load profile given in [34] to mimic a more realistic scenario. From this figure, it is quite evident that the voltage profile of the system is within the specified boundaries, i.e. [0.93 p.u. − 1.03 p.u.].

C. ACHIEVABLE SYSTEM PROFIT

We now compare **GreedyMCS** with **RandomMCS** in terms of social welfare of the system by adjusting the weighting parameter (δ). The results obtained by changing parameter δ from 0 to 1 with a step-size of 0.1 are shown in Fig. 6(a). As seen from the results, **GreedyMCS** outperforms the baseline algorithm by nearly 30%, on average, for different δ values. This is because our algorithm takes advantage of the updating heuristics to tactfully forward each vehicle to the most profitable CS.

In addition to the social welfare, behavior analysis of the algorithms in sharing the profits between both, EVs and CSs under varying δ values is also imperative. Fig. 6(b) plots the net profit jointly earned by the EV owners and CSs for varying δ values. Unlike the baseline solution, **GreedyMCS** allocates EVs to CSs in a way that each entity relatively achieves the maximum profit based on δ. Particularly, when using **GreedyMCS** for EV scheduling, EV owners gain higher profit for $\delta < 0.5$, whereas for $\delta > 0.5$, the CSs make more profit. Therefore, selection of an appropriate δ that minimizes the profit loss on each side is critical to the local schedulers. For instance, it can be observed from Fig. 6(b) that $\delta = 0.4$ results in a minimum profit of approximately $\$350$ for CSs with at most $\$2,200$ profit loss for the EV owners. Conversely, a minimum profit of about $\$500$ can be achieved for CSs with little loss in EV profit when $\delta = 0.6$. It goes without saying that results of Fig. 6 alongside the EV arrival patterns, which is learned by aggregators over time, and the profit interests of each entity in the system can be used as guidelines by aggregators to decide on the most suitable value for δ in online scheduling scenarios.

Under tight constraints on the EV service type and their profit interests, Fig. 7 shows how the rise in EV population can compensate for the increase in battery costs. For this simulation scenario, we only consider EVs demanding for discharging service with the interest in maximizing

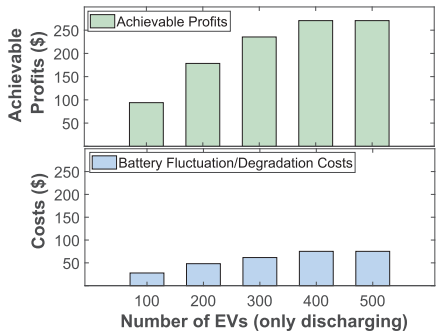

FIGURE 7. Comparison of obtainable EV profits against the associated battery costs.

their own profits (i.e., $\delta = 0$). This figure clearly showcases the achievable EV profits and the related battery fluctuation/degradation costs. As can be observed, the growth in EV profit by increasing their number from 100 to 500 compensates for the rise in associated battery costs by an average of about 2.5 times higher in terms of profits. Obviously, this observation confirms the robustness of proposed model in motivating EVs for participation in the DR program.

D. COMPUTATION TIME

The **GreedyMCS** and **RandomMCS** algorithms are now compared in terms of computation time for different number of EVs and under fixed number of CSs. Fig. 8 compares the worst-case time complexity for a large-scale network of EVs. In this figure, the comparison results are shown for number of EVs varying from 10^3 to 10^4 and 10 CSs. Another parameter that impacts the complexity of the algorithms is the time taken to solve the local optimization problem of (24). In other words, the computation time for both algorithms shown in Fig. 8 are in terms of EV population and time value t_{opt} (in millisecond) which varies from 10ms to 100ms (depending on the underlying hardware).

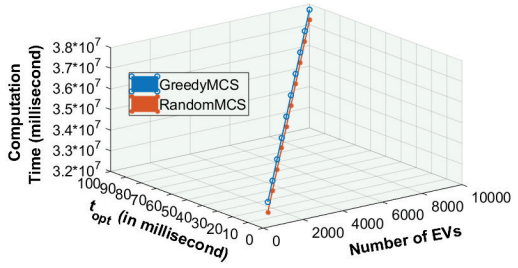

FIGURE 8. Comparison between GreedyMCS an RandomMCS algorithms in terms of computation time.

As seen in Fig. 8, **GreedyMCS** surges with the same order of complexity as **RandomMCS** under fixed number of CSs and dramatic increase in the EV population. This is due to the dominating role of the number of CSs in the complexity of **GreedyMCS**. In practice, since the increase in EV population is indubitably higher than the number of deployed CSs, both algorithms achieve the same rate of computation time as the number of EVs increases substantially. Therefore, our proposed algorithm enhances the social welfare of the system (Fig. 6(a)) with the same rate of complexity growth as compared to its counterpart. It should be also noted that in very large-scale EV scheduling, the computational time can be greatly reduced in practical scenarios using high powerful processors as schedulers at the aggregators.

E. IMPACT OF EV POPULATION AND DEPARTURE TIME

Next, we investigate the profits achievable by each participant in the system under the influence of the EV fleet size and their home departure times. Depending on penetration type, it is interesting to observe how the EV population in energy distribution system affects their obtainable profits and whether it compensates for the increase in auxiliary costs.

Fig. 9 demonstrates the impact of the number of EVs on the overall system profit that can be earned. With increase in the number of EVs from 500 to 1000 Fig. 9(a), we observe that the achievable profit decreases when $\delta = 0$ (i.e., only EV profit is considered). Such behavior arises due to the fact that higher penetration of EVs with charging service type causes the real-time electricity price to increase which subsequently, reduces the revenue obtained by the EV fleet from their charging service. In contrast, CSs on the other hand obtain higher profits (when $\delta = 1$) as EVs pay more for the charging service.

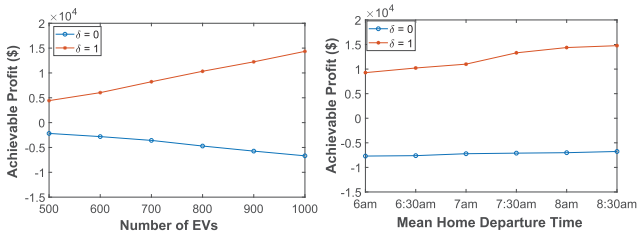

FIGURE 9. Achievable system profits impacted by (a) the number of EVs and (b) their home departure times.

The impact of changing the time of EV home departures on the overall achievable system profit is shown in Fig. 9(b). By fixing the number of EVs to 1000, the figure marks the simulation results for six different home departure times (mean of uniform distribution). The profit of both EVs and CSs increases with larger mean home departure time because when the mean of home departure time increases, more charging and discharging EV loads are shifted to low and high base loads on the grid, respectively, which in turn, improves the profit made by EVs. Likewise, CSs will also have more flexibility in offering charging/discharging prices that not only favor the EVs, but also result in improving their own profits. Moreover, Fig. 9(b) reveals that increase in EV profit is lesser compared to that for CSs. The results in Fig. 9(a) and Fig.9(b) imply that increasing the EV penetration tends to effectively boost the achievable profits for CSs.

F. IMPACT OF CS SCALABILITY AND V2G PENETRATION

In addition to the density of EVs in the energy distribution system, it is also compelling to analyze how increasing the number of deployed CSs and increasing the percentage of EVs participating in the V2G program can affect the obtainable profits for both system participants. Based on these observations, the V2G system designer can accordingly invest on the optimal deployment of CSs or V2G penetration.

With regard to this objective, we scrutinize the effect of the number of deployed CSs in the distribution system on the overall obtainable profit. By increasing the number of CSs from 10 to 110, the total system profit is boosted for $\delta = 0$ as shown in Fig. 10(a). This tells us that with increase in CSs, the vehicles find wider options in selecting a CS yielding higher profit for charging operations. Nevertheless, for $\delta = 1$, the profit that the CSs obtain drops when their number increases; although the CSs obtain higher revenue in the presence of more number of stations, their associated auxiliary costs grows relatively higher which in turn, reduces their net profit. As seen in Fig. 10(a), the profit growth is very small when more than 70 CSs are deployed, which confirms it as the optimal number of stations to be deployed in the distribution system for this particular set-up.

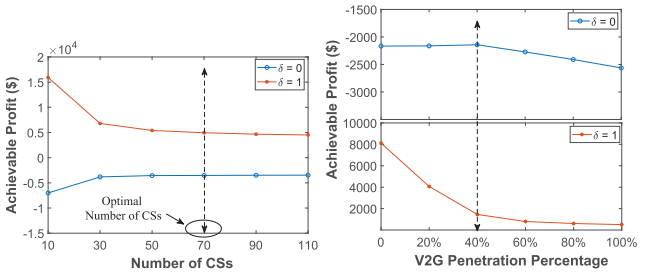

FIGURE 10. Achievable system profit under the impact of (a) the number of deployed CSs and (b) the percentage of V2G penetration.

The impact of increasing the penetration percentage of EVs belonging to M^{V2G} is depicted in Fig. 10(b), where 1000 EVs and 10 CSs are considered. The V2G penetration increases up to 100%, while the remaining penetration percentage of EVs is equally divided between EVs with only charging and only discharging demands. For instance, when V2G penetration is at 40%, the penetration of EVs with only charging and discharging demand is equally 30%. As observed for $\delta = 0$, the overall profit initially increases due to the two-way energy exchange between EVs and the power grid as an ancillary service. However, the overall profit gradually drops as δ approaches 1. This is because the total revenue of CSs reduces as they have to pay more to the increasing number of EVs for the energy they return back to the power grid. Also note that for $\delta = 0$, the overall profit falls beyond an optimal V2G penetration point. In Fig. 10(b), this optimal penetration percentage is shown to be around 40%. The reason is that increasing the influx of EVs with V2G service needs increases the EV battery fluctuation costs due to consecutive charging/discharging operations after some point which consequently, results in profit reduction.

G. POWER GRID ANCILLARY SERVICES

In this sub-section, we examine the ancillary services, namely the peak load reduction and load shifting, provided to the power grid using our algorithm. An advantage of the DR program is the participation of EVs in V2G operation and the ability to return back the stored energy in their battery to the power grid during the peak-load hours in order to improve the grid stability. To verify this advantage through simulation, we first investigate the impact of EV penetration percentage with V2G type on peak load reduction using **GreedyMCS**. For this simulation, we considered 20% and 30% penetration levels, $\delta = 0$, EV departure time chosen from the uniform interval U[8 a.m., 10 a.m.], and the stay duration at CSs selected from interval U[6 hrs, 9 hrs].

The average peak reduction percentage over the time interval 10 a.m. to 6 p.m. at all CSs is shown in Fig. 11. Note that following the definition in [5], the peak load reduction percentage within a given time period at any station is derived as the gap between the highest base load and the maximum load created by the algorithm over the period at the station. The results in Fig. 11 reveal that further peak load reduction can be achieved by increasing the penetration of V2G vehicles since they sell their battery energy to the grid during peak electricity demands. In here, average peak reductions of 14.32% and 26% are achieved for the penetration levels of 20% and 30%, respectively, during the given time interval. In practical scenarios, the planning of V2G penetration during different times of the day can be decided by system designers depending on the desired percentage of peak load reduction.

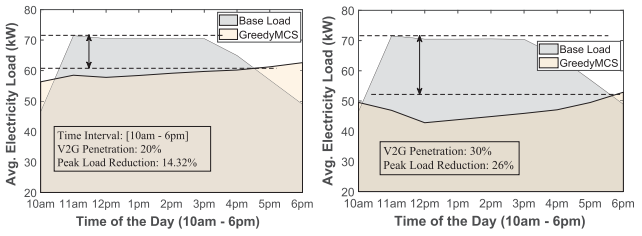

FIGURE 11. Impact of V2G penetration on average peak load reduction for (a) 20% and (b) 30% penetration levels.

Finally, the comparison between **GreedyMCS** and **RandomMCS** in terms of the final mean load accumulated on the grid (load shifting) at all CSs within the time interval [3 p.m., 9 p.m.] when $\delta = 0$ is tabulated in Table 3. Here, 50% of EVs require only charging and the remaining 50% are interested in only discharging energy. Also, the home departure time is taken from U[1 a.m., 12 p.m.] and the time duration spent at the CSs is similar to the preceding scenario.

We note that the root mean square deviation (*rmsd*) of the generated load by an algorithm from the highest base load over a given time period is used as the criteria for load

TABLE 3. Single day average load shifting at all CSs.

Time	Max. Base Load	GreedyMCS	RandomMCS
3 p.m.	70.4851 kW	66.2857 kW	57.8363 kW
4 p.m.	70.4851 kW	66.2751 kW	57.8314 kW
5 p.m.	70.4851 kW	65.9560 kW	57.8162 kW
6 p.m.	70.4851 kW	65.1286 kW	57.3847 kW
7 p.m.	70.4851 kW	60.8431 kW	53.7086 kW
8 p.m.	70.4851 kW	49.7638 kW	47.2927 kW
9 p.m.	70.4851 kW	33.9434 kW	32.3213 kW

shifting at any station [5]. From the data in Table 3, the *rmsd* values of 16.65 and 20.45 are obtained for **GreedyMCS** and **RandomMCS** algorithms, respectively, during the time interval [3 p.m., 9 p.m.]. Therefore, we conclude that our greedy-based approach is superior in terms of flattening the final grid electricity load as compared to the uncontrolled random counterpart. This is because **GreedyMCS** allocates the EV charging demands to the time intervals with low electricity load on the power grid in a controlled manner in order to maximize the obtainable profit. Ultimately, this helps to shift the charging load to the valley intervals and avoid power grid overloading during peak hours. Averaged over all CSs, an improvement of nearly 20% in load shifting during the above time interval is achieved when our algorithm is adopted. It is worth mentioning that the advantage of effective load shifting brought by our algorithm is more valuable in large-scale EV networks with charging demands.

VII. DISCUSSIONS

As the main challenge in real-world implementation of the proposed distributed EV scheduling algorithm, one may refer to the proper adjustment of the weighting parameter δ by the aggregators. In practice, this adjustment can be learned by aggregators over the system operational period. The learning process can utilize the parameters such as the daily commute patterns of EVs and their profit interests in order to improve the efficiency. The sub-optimality of the algorithm can be pointed out as another limitation of the proposed model. The generation of efficient near-optimal solutions with fast computational performance reasonably compensates for this limitation specially in large-scale energy distribution systems where fast solutions are preferred by system designers rather than optimal solutions.

Factors such as very high uncertainty in EV commuting patterns and their energy demand or the unexpected environmental impacts on EV battery fluctuation and degradation costs may slightly affect the measurement confidence of 90% for our obtained results in practice. Despite of such factors, this high confidence interval obviously confirms the suitability of our results as some guidelines for V2G distribution system designers in practical scenarios. Using these findings, the aggregators can agree on an appropriate value for δ where the desired amount of profits is obtained for both EVs and CSs depending on EV density and the type of their participation in V2G operations. In addition, system designers can effectively adjust the EV population and particularly, V2G penetration in real-world scenarios to attain the desired peak-load reduction or load shift as the ancillary services for the power grid.

VIII. CONCLUSION AND FUTURE WORK

Motivated by smart city applications, this paper investigated the decentralised scheduling of EVs in a large-scale smart energy distribution system comprising of multiple spatially-located CSs, each managed by individual aggregators. The proposed scheme offers high flexibility in CS selection for EVs with different service preferences. From the aspect of V2G management, a mixed integer non-linear programming (MINLP) optimization problem was formulated to generalize existing social welfare maximization models. Indeed, a distributed online greedy-based scheduling algorithm with low-complexity was proposed to adjust the overall achievable profit and efficient updating heuristics were adopted to tactfully guide each EV to the most profitable CS. The proposed algorithm reduces the original MINLP model to a non-linear programming model and then determines the energy exchange between EV and CS with the provision of desired grid ancillary services by taking advantage of a root mean square deviation based optimizer at each CS. The superiority of the proposed algorithm with respect to a baseline solution was verified through simulations conducted on the IEEE 37 bus distribution network. Particularly, an average 30% improvement in social welfare of the system was achieved using our algorithm under equal participation of EVs in charging and discharging services. Considering the best-case performance, where the maximization of only EVs profit is concerned, the final electricity load on the power grid was further flattened by up to 20%. Based on the system configuration, our results further revealed the existence of an optimal number of CSs to be deployed which is key to optimizing investments for large-scale distributed energy management in smart cities.

Due to their limited processing capacity, the aggregators in V2G systems stand the risk of being overloaded with large number of EV requests. As an interesting extension to this work, mobile edge computing could be exploited to address this issue in large-scale EV charging/discharging scheduling. Integration of renewable energy with CSs and efficient electricity load management mechanisms are other promising research directions relevant to social welfare maximization.

REFERENCES

[1] T. G. Alghamdi, D. Said, and H. T. Mouftah, "Decentralized electric vehicle supply stations (D-EVSSs): A realistic scenario for smart cities," *IEEE Access*, vol. 7, pp. 63016–63026, 2019.

[2] J. C. Mukherjee and A. Gupta, "A review of charge scheduling of electric vehicles in smart grid," *IEEE Syst. J.*, vol. 9, no. 4, pp. 1541–1553, Dec. 2015.

[3] E. Vega-Fuentes and M. Denai, "Enhanced electric vehicle integration in the UK low-voltage networks with distributed phase shifting control," *IEEE Access*, vol. 7, pp. 46796–46807, 2019.

[4] P. Wang, S. Zou, and Z. Ma, "A partial augmented Lagrangian method for decentralized electric vehicle charging in capacity-constrained distribution networks," *IEEE Access*, vol. 7, pp. 118229–118238, 2019.

[5] Z. Wang and S. Wang, "Grid power peak shaving and valley filling using Vehicle-to-Grid systems," *IEEE Trans. Power Del.*, vol. 28, no. 3, pp. 1822–1829, Jul. 2013.
[6] W. Tang, S. Bi, and Y. J. Zhang, "Online coordinated charging decision algorithm for electric vehicles without future information," *IEEE Trans. Smart Grid*, vol. 5, no. 6, pp. 2810–2824, Nov. 2014.
[7] R. Yu, W. Zhong, S. Xie, C. Yuen, S. Gjessing, and Y. Zhang, "Balancing power demand through EV mobility in vehicle-to-grid mobile energy networks," *IEEE Trans. Ind. Informat.*, vol. 12, no. 1, pp. 79–90, Feb. 2016.
[8] P. You, Z. Yang, M.-Y. Chow, and Y. Sun, "Optimal cooperative charging strategy for a smart charging station of electric vehicles," *IEEE Trans. Power Syst.*, vol. 31, no. 4, pp. 2946–2956, Jul. 2016.
[9] E. Yao, V. W. S. Wong, and R. Schober, "Robust frequency regulation capacity scheduling algorithm for electric vehicles," *IEEE Trans. Smart Grid*, vol. 8, no. 2, pp. 984–997, Mar. 2017.
[10] A. Mehrabi and K. Kim, "Low-complexity charging/discharging scheduling for electric vehicles at home and common lots for smart households prosumers," *IEEE Trans. Consum. Electron.*, vol. 64, no. 3, pp. 348–355, Aug. 2018.
[11] H. Mohsenian-Rad and M. Ghamkhari, "Optimal charging of electric vehicles with uncertain departure times: A closed-form solution," *IEEE Trans. Smart Grid*, vol. 6, no. 2, pp. 940–942, Mar. 2015.
[12] J. C. Mukherjee and A. Gupta, "Distributed charge scheduling of plug-in electric vehicles using inter-aggregator collaboration," *IEEE Trans. Smart Grid*, vol. 8, no. 1, pp. 331–341, Jan. 2017.
[13] S.-A. Amamra and J. Marco, "Vehicle-to-Grid aggregator to support power grid and reduce electric vehicle charging cost," *IEEE Access*, vol. 7, pp. 178528–178538, Dec. 2019.
[14] X. Wang, C. Sun, R. Wang, and T. Wei, "Two-stage optimal scheduling strategy for large-scale electric vehicles," *IEEE Access*, vol. 8, pp. 13821–13832, 2020.
[15] S. Pal and R. Kumar, "Electric vehicle scheduling strategy in residential demand response programs with neighbor connection," *IEEE Trans. Ind. Informat.*, vol. 14, no. 3, pp. 980–988, Mar. 2018.
[16] F. Luo, J. Zhao, Z. Y. Dong, Y. Chen, Y. Xu, X. Zhang, and K. P. Wong, "Cloud-based information infrastructure for next-generation power grid: Conception, architecture, and applications," *IEEE Trans. Smart Grid*, vol. 7, no. 4, pp. 1896–1912, Jul. 2016.
[17] D. A. Chekired and L. Khoukhi, "Smart grid solution for charging and discharging services based on cloud computing scheduling," *IEEE Trans. Ind. Informat.*, vol. 13, no. 6, pp. 3312–3321, Dec. 2017.
[18] D. A. Chekired, L. Khoukhi, and H. T. Mouftah, "Decentralized cloud-SDN architecture in smart grid: A dynamic pricing model," *IEEE Trans. Ind. Informat.*, vol. 14, no. 3, pp. 1220–1231, Mar. 2018.
[19] X. Hu, K. Wang, X. Liu, Y. Sun, P. Li, and S. Guo, "Energy management for EV charging in software-defined green Vehicle-to-Grid network," *IEEE Commun. Mag.*, vol. 56, no. 5, pp. 156–163, May 2018.
[20] A. Ahmadian, M. Sedghi, M. Aliakbar-Golkar, M. Fowler, and A. Elkamel, "Two-layer optimization methodology for wind distributed generation planning considering plug-in electric vehicles uncertainty: A flexible active-reactive power approach," *Energy Convers. Manage.*, vol. 124, pp. 231–246, Sep. 2016.
[21] A. Ahmadian, M. Sedghi, B. Mohammadi-ivatloo, A. Elkamel, M. A. Golkar, and M. Fowler, "Cost-benefit analysis of V2G implementation in distribution networks considering PEVs battery degradation," *IEEE Trans. Sustain. Energy*, vol. 9, no. 2, pp. 961–970, Apr. 2018.
[22] M. A. Mirzaei, A. S. Yazdankhah, B. Mohammadi-Ivatloo, M. Marzband, M. Shafie-khah, and J. P. S. Catalão, "Stochastic network-constrained co-optimization of energy and reserve products in renewable energy integrated power and gas networks with energy storage system," *J. Cleaner Prod.*, vol. 223, pp. 747–758, Jun. 2019.
[23] H. J. Monfared, A. Ghasemi, A. Loni, and M. Marzband, "A hybrid price-based demand response program for the residential micro-grid," *Energy*, vol. 185, pp. 274–285, Oct. 2019.
[24] K. Chaudhari, A. Ukil, K. N. Kumar, U. Manandhar, and S. K. Kollimalla, "Hybrid optimization for economic deployment of ESS in PV-integrated EV charging stations," *IEEE Trans. Ind. Informat.*, vol. 14, no. 1, pp. 106–116, Jan. 2018.
[25] A. Schrijver, *Theory of Linear and Integer Programming*. Chichester, U.K.: Wiley, 2000.
[26] J. Valinejad, T. Barforoshi, M. Marzband, E. Pouresmaeil, R. Godina, and J. P. S. Catalão, "Investment incentives in competitive electricity markets," *Appl. Sci.*, vol. 8, no. 10, p. 1978, Oct. 2018.
[27] T. H. Cormen, C. E. Leiserson, R. L. Rivest, and C. Stein, *Introduction to Algorithms*. Cambridge, MA, USA: MIT Press, 2009.
[28] M. Ghofrani, A. Arabali, M. Etezadi-Amoli, and M. S. Fadali, "Smart scheduling and cost-benefit analysis of grid-enabled electric vehicles for wind power integration," *IEEE Trans. Smart Grid*, vol. 5, no. 5, pp. 2306–2313, Sep. 2014.
[29] A. Ahmadian, M. Sedghi, A. Elkamel, M. Fowler, and M. Aliakbar Golkar, "Plug-in electric vehicle batteries degradation modeling for smart grid studies: Review, assessment and conceptual framework," *Renew. Sustain. Energy Rev.*, vol. 81, pp. 2609–2624, Jan. 2018.
[30] A. Mehrabi and K. Kim, "General framework for network throughput maximization in sink-based energy harvesting wireless sensor networks," *IEEE Trans. Mobile Comput.*, vol. 16, no. 7, pp. 1881–1896, Jul. 2017.
[31] W. Tushar, C. Yuen, S. Huang, D. B. Smith, and H. V. Poor, "Cost minimization of charging stations with photovoltaics: An approach with EV classification," *IEEE Trans. Intell. Transp. Syst.*, vol. 17, no. 1, pp. 156–169, Jan. 2016.
[32] M. Grant and S. Boyd. (Mar. 2014). *CVX: MATLAB Software for Disciplined Convex Programming, Version 2.1*. [Online]. Available: http://cvxr.com/cvx
[33] L. P. Fernández, T. G. S. Roman, R. Cossent, C. M. Domingo, and P. Frías, "Assessment of the impact of plug-in electric vehicles on distribution networks," *IEEE Trans. Power Syst.*, vol. 26, no. 1, pp. 206–213, Feb. 2011.
[34] H. S. V. S. K. Nunna and D. Srinivasan, "Multiagent-based transactive energy framework for distribution systems with smart microgrids," *IEEE Trans. Ind. Informat.*, vol. 13, no. 5, pp. 2241–2250, Oct. 2017.

ABBAS MEHRABI (Member, IEEE) received the B.Sc. degree in computer engineering from the Shahid Bahonar University of Kerman, Kerman, Iran, in 2008, the M.Sc. degree in computer engineering from Azad University, South Tehran, Iran, in 2010, and the Ph.D. degree from the School of Electrical Engineering and Computer Science, Gwangju Institute of Science and Technology, Gwangju, South Korea, in 2017. From 2017 to 2019, he was a Postdoctoral Researcher with the Department of Computer Science, Aalto University, Espoo, Finland. He is currently a Lecturer with the Department of Computing and Technology, Nottingham Trent University, Nottingham, U.K. His research interests include quality of experience optimization and resource allocation in mobile edge computing environments, the Internet of Things, vehicular fog computing, and scheduling/planning problems in smart grids.

H. S. V. S. KUMAR NUNNA (Member, IEEE) received the B.Tech. degree in electrical and electronics engineering from Jawaharlal Nehru Technological University Hyderabad (JNTUH), India, in 2007, the M.Tech. degree in industrial power and automation (formerly known as computer controlled industrial power) from the National Institute of Technology, Calicut, India, in 2010, and the Ph.D. degree in power and energy systems from IIT Bombay, Mumbai, India, in 2014. From January 2015 to June 2017, he was a Postdoctoral Fellow with the Green Energy Management and Smart Grid Research Center, National University of Singapore (NUS). From July 2014 to January 2015, he was also a Research Associate with the Department of Energy Science and Engineering, IIT Bombay. Since September 2017, he has been working as an Assistant Professor with the School of Engineering and Digital Sciences, Nazarbayev University, Nur-Sultan, Kazakhstan. His current research interests are transactive energy systems, microgrids, electricity markets, and multiagent system applications to power and energy systems.

ARESH DADLANI (Member, IEEE) received the B.Sc. and M.Sc. degrees in electrical and computer engineering from the University of Tehran, Tehran, Iran, in 2007 and 2010, respectively, and the Ph.D. degree from the School of Information and Communications, Gwangju Institute of Science and Technology (GIST), Gwangju, South Korea, in 2015. From 2008 to 2010, he was with the School of Computer Science, Institute for Studies in Theoretical Physics and Mathematics (IPM), Tehran, Iran, as a Research Assistant. From 2015 to 2017, he was with the Center for Integrated Access Systems, Gwangju, South Korea as a Postdoctoral Researcher. Since September 2017, he has been with the School of Engineering and Digital Sciences, Nazarbayev University, Nur-Sultan, Kazakhstan, where he is currently an Assistant Professor and the Director of the Complex Networks and Systems Group. His research interests include modeling and analysis of complex system dynamics, network science, and applications of optimization techniques and modern queuing theory in wireless communication networks.

SEUNGPIL MOON received the B.Sc., M.Sc., and Ph.D. degrees in electrical engineering from Gyeongsang National University in 1996, 1998, and 2003, respectively. His research interests include probabilistic production cost simulation, reliability evaluation, and outage cost assessment of power systems and economic operations of power systems. He is currently a Senior Researcher with the Korea Electric Power Corporation Research Institute (KEPRI), Daejeon, South Korea.

KISEON KIM (Senior Member, IEEE) received the B.Eng. and M.Eng. degrees in electronics engineering from Seoul National University, Seoul, South Korea, in 1978 and 1980, respectively, and the Ph.D. degree in electrical engineering systems from the University of Southern California at Los Angeles, Los Angeles, CA, USA, in 1987. From 1988 to 1991, he was with Schlumberger, Houston, TX, USA. From 1991 to 1994, he was with the Superconducting Super Collider Laboratory, Waxahachie, TX, USA. In 1994, he joined the Gwangju Institute of Science and Technology, Gwangju, South Korea, where he is currently a Professor. His current research interests include wideband digital communications system design, sensor network design, analysis and implementation both at the physical and at the resource management layer, and biomedical application design. He is a member of the National Academy of Engineering of Korea, a Fellow of the IET, and a Senior Editor of the IEEE SENSORS JOURNAL.